NEURONAL AVALANCHES FOR EEG-BASED MOTOR IMAGERY BCI

C. Mannino[1], P. Sorrentino[2,3], M. Chavez[1], M.-C. Corsi[1]

[1]Sorbonne Université, Institut du Cerveau – Paris Brain Institute -ICM, CNRS, Inria, Inserm,
AP-HP, Hôpital de la Pitié Salpêtrière, F-75013, Paris, France
[2]Institut de Neurosciences des Systèmes, Aix-Marseille Université, 13005 Marseille, France
[3]University of Sassari, Department of Biomedical Sciences, Viale San Pietro, 07100, Sassari, Italy

E-mail: marie-constance.corsi@inria.fr

ABSTRACT:
Current features used in motor imagery-based Brain-Computer Interfaces (BCI) rely on local measurements that miss the interactions among brain areas. Such interactions can manifest as bursts of activations, called neuronal avalanches. To track their spreading, we used the avalanche transition matrix (ATM), which contains the probability that an avalanche would consecutively recruit any two brain regions. Here, we proposed to use ATMs as a potential alternative feature. We compared the classification performance resulting from ATMs to a benchmark model based on Common Spatial Patterns.
In both sensor-and source-spaces, our pipeline yielded an improvement of the classification performance associated with reduced inter-subject variability. A correspondence between the selected features with the elements of the ATMs that showed a significant condition effect led to higher classification performance, which speaks to the interpretability of our findings.
In conclusion, working in the sensor space provides enough spatial resolution to classify. However the source space is crucial to precisely assess the involvement of individual regions.

INTRODUCTION

Neuroscientists have been exploring and researching Brain-Computer Interface (BCI) since the70s as a way to restore communication and motor capabilities for severely disabled people., such as patients affected by amyotrophic lateral sclerosis, stroke, or spinal cord injury [1].
In non-invasive BCI, Event Related Desynchronization/Synchronization, Event Related Potentials, and Steady State Evoked Potentials are the most informative brain activity patterns for communication and control applications to design electroencephalography (EEG)-based BCI. One of the main drawbacks of the current systems lies in the high inter/intra-subject variability, notably in terms of performance. Indeed, multiple studies reported that 15%–30% of the subjects fail in controlling a BCI device. This is a phenomenon referred to as the "BCI inefficiency" [2]. Among the potential causes are the selected data features. Indeed, relying mostly on local measurements might not effectively capture brain functioning, as some information is encoded in the interactions between areas [3].
To overcome these limitations and to take advantage of the EEG time-resolution, in a recent work, we proposed to use a metric that captures the dynamic nature (i.e. changing in space and time) of the brain activities: the neuronal avalanches. Neuronal avalanches are characterised by the propagation of cascading bursts of activity [4]. Previous studies show that their spreading preferentially across the white-matter bundles [5] and that neuronal cascades are a major determinant of spontaneous fluctuations in brain dynamics at rest [6]. Furthermore, in our previous work we showed that neuronal avalanches, estimated from source-reconstructed data, spread differently according to the task performed by the user, demonstrating the potential relevance of neuronal avalanches as an alternative feature for detecting the subjects' intent [7].
Here, we investigated to which extent this framework would be compatible with a BCI experiment. For this purpose, instead of working in the source domain that requires additional data (e.g. individual magnetic resonance imaging) and computational resources, we tested the performance of neuronal avalanches directly in the sensor domain. Indeed, the methodological validity of sensor space measures is especially relevant for online studies in a clinical setting due to time and economic constraints. We hypothesised that despite a reduction of the spatial resolution, using the neuronal avalanches in the sensor space could help in classification performance, and that the selected features could be neurophysiologically interpretable and relevant.

MATERIALS AND METHODS

Participants

The research was conducted in accordance with the Declaration of Helsinki. A written informed consent was obtained from subjects after explanation of the study, which was approved by the ethical committee CPP-IDF-VI of Paris. All participants received financial compensation at the end of their participation. Twenty healthy subjects (27.5 ± 4.0 years old, 12 men), with no medical or psychological disorder, were recruited.

Experimental protocol

The dataset used in our study originates from Corsi et al. [8] and involves a BCI task structured around a two-target box task. Participants were required to adjust their brain's alpha and/or beta activity levels to control a cursor's vertical movement, aiming to reach a vertical bar, referred to as a target displayed on the screen. Achieving the upper target necessitated the subjects to engage in continuous motor imagery (MI) of right-hand

grasping. Conversely, reaching the lower target required the subjects to remain in a resting state. Each session comprised 32 trials, evenly and randomly split between the up and down targets, correlating with the MI and Rest conditions, respectively. For a complete description of the protocol, the reader can refer to [8].

EEG data acquisition & pre-processing
EEG data were captured using a 74-channel EEG system equipped with Ag/AgCl passive sensors (Easycap, Germany), arranged according to the 10-10 standard montage. Reference electrodes were placed on the mastoids, with the ground electrode on the left scapula. Recordings took place in a magnetically shielded room, utilising a 0.01-300Hz bandwidth and sampling at 1kHz. Two channels (namely T9 and T10) were identified as bad and rejected based on the amplitude of the signals recorded, with a threshold of three standard deviations. For a complete description of the pre-processing steps, please refer to [8].

Neuronal Avalanches extraction
The neuronal avalanches analysis consists of identifying large signal excursions beyond a given threshold. The cascades are captured by clustering these discrete supra-threshold events based on temporal proximity, thus, defining neuronal avalanches as periods of collective spatio-temporal organization. Each signal was z-scored (over time), and set to 1 when above a threshold, and to 0 otherwise. An avalanche was defined as starting when at least one channel is above threshold (referred here as active channel), and as finishing when all channels were inactive [4,5,6]. For each avalanche, we estimated a transition matrix A, called Avalanche Transition Matrix (ATM), structured with channels in rows and columns, and the ijth element of matrix A defined as the probability that the electrode j would be active at time t+1, given the electrode i was active at time t. For each subject, we obtained a transition matrix over all avalanches for each condition (MI and Rest conditions).

Classification Analysis
To explore the applicability of the ATM method in the context of a BCI training, we performed a subject-specific analysis.
The classification step was done using a Support Vector Machine (SVM). To assess the extent to which the ATMs might be considered as an alternative feature for BCIs, we compared our approach (ATM+SVM) to a framework that relies on spatial filters, namely Common Spatial Patterns (CSP+SVM) [9, 10].
For each approach (namely ATM+SVM or CSP+SVM), we classified different tasks at the individual level. To evaluate the classification performance, we divided the dataset to include 80% of the trials in the train split and 20% of the trials in the test split. The classification scores for all pipelines were evaluated with an accuracy measurement using a random permutation cross-validator. To assess the robustness of our framework, we also tested a different number of re-shuffling & splitting iterations (5/25/50/75).

For each subject, the CSP method decomposes signals using spatial filters, and then selects the n modes that capture the highest inter-class variance. Here, we selected eight spatial modes and returned the average power of each.
As for the ATMs, to consider the subjects' specificity, we optimised two parameters, namely: the threshold applied to the z-scored signals (ranging from 1.0 to 4.0), and the minimal duration of the considered avalanches (ranging from 2 to 8) [11]. Inside the ATM pipeline the choice of the best decoding parameters relied on a posteriori classification accuracy performance rate.
Finally, we individually compared the classification performance obtained with the CSP+SVM and with the ATM+SVM approaches, respectively. We run t-tests under the null hypothesis that, for a given subject, CSP+SVM and ATM+SVM would not yield statistically significant differences in classification. We repeated the comparison for all the subjects and corrected these statistical comparisons for multiple comparisons across subjects using the False Discovery Rate (FDR) [12]. Such an analysis has been performed across 25, 50, and 75 splits. However, given its poor statistical power, it is not possible to apply a statistical test over 5 splits classification. Therefore, to evaluate whether the difference between the two pipelines could be considered as significant, we calculated the averaged classification performance across splits using both CSP+SVM and ATM+SVM and we determined the difference for each subject. Ultimately, we compared the absolute value of the difference with our predefined threshold, considering the classification performance not statistically different if the magnitude of the difference between the two methods was less than a threshold. We established the threshold at an arbitrary value of 0.05. As a sanity check, we performed this analysis in the source space, as we did in [7]. For a complete description of the source-reconstruction steps, the reader can refer to [8].

In this work, we used preprocessed signals that were bandpass filtered between 3 and 40Hz. To investigate the potential effect induced by the choice of the frequency band, we performed the same analysis in the μ band (8 – 13 Hz) and in the beta band (13 – 30 Hz) [not shown]. We performed a one way ANOVA (df = 2) among these three-frequency bands under the null hypothesis (H0) that these groups came from the same population. For both approaches (CSP+SVM and ATM+SVM), no frequency band effect on the classification performance was observed (p-value > 0.05). Therefore, in the next sections, we will report the results were obtained within the 3-40 Hz band.

Decoding: Features importance analysis
To investigate the interpretability of the classification performance, we examined the relative importance of the features derived from the absolute values of the classification coefficients in the model. To better understand the features importance across subjects, we carried out a quantitative reliability analysis across the cohort to identify the repetition of the selected features in
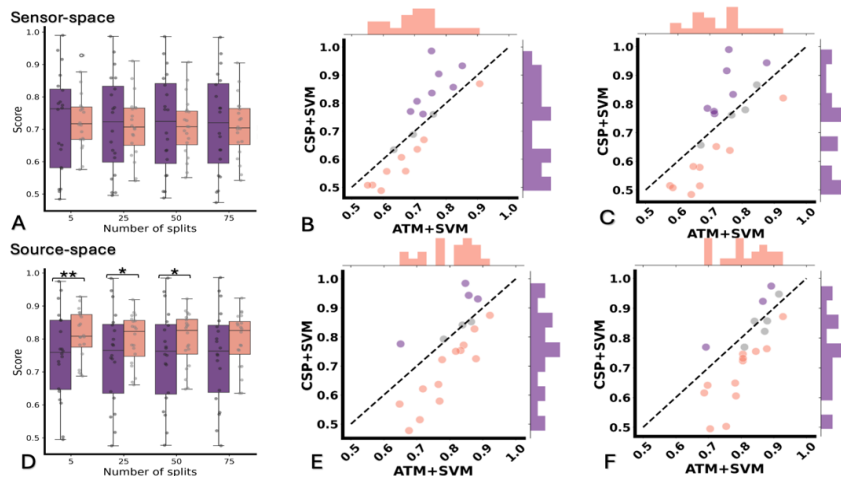
Figure 1: Classification performance. (A/D) *Effect of splits tested on ATM+SVM and CSP+SVM at group level in sensor-space (A) and source-space (D).* **(B/E)** *Individual level classification performance in sensor-space (B) and source-space (E) using 50 random splits.* **(D/F)** *Individual level classification performance in sensor-space (D) and source-space (F) using 5 random splits. Color coded: in salmon, ATM+SVM pipeline; in violet, CSP+SVM pipeline. Statistical difference between CSP + SVM & ATM + SVM: * pval < 0.05, ** pval < 0.01.*

at least half of the subjects. To investigate features importance from a nodal point of view we set as a threshold the median value across channels and subjects, then we evaluated which nodes were over threshold in the majority of the subjects. We computed this analysis over the entire dataset (20 subjects) but also independently on two different sub-groups: on the 10 most responsive subjects according to ATM classification performance and on the 10 least responsive subjects respectively. All these investigations were also performed in the source space.

Encoding: Quantification and statistical analysis
To identify the edges (i.e. functional links) that are more likely to be recruited during a hand motor imagery task as compared to resting state, for each participant, we calculated the variance in the probability of perturbations traversing a specific edge between resting state and MI task. To assess the statistical significance, we randomized the labels of individual avalanches for each person. This shuffling was repeated 10,000 times to generate a distribution of differences for each edge under the null hypothesis that the transition matrices revealed no distinction between the two conditions. We then determined statistical significance for each edge against this null distribution, applying Benjamini-Hochberg correction for multiple comparisons across edges. This process yielded a matrix for each subject, highlighting $S_{i,j}$ values (here referred to as edges) with statistically significant differences between conditions. We assessed the consistency of these matrices across individuals, concentrating on edges consistently implicated in the task. Then, we performed a node-wise analysis to identify the nodes over which significant differences were clustered. These nodes were referred to as "task-specific" areas.

RESULTS
Classification performance
Working on the entire dataset of 20 subjects, as a

standard configuration, we used 50 random splits.

At the group-level, the classification performance in the sensor space, between CSP+SVM and ATM+SVM is similar (t-test, pval > 0.05). Nevertheless, we observed a larger inter-subject variability with CSP+SVM (71%+/15%) as compared to ATM+SVM (71% +/- 9%). In the source-space, ATM+SVM (80%+/-8%) led to a statistical improvement of the classification performance as compared to CSP+SVM (75%+/-14%) (t-test, pval<0.05) such as a reduced inter-subject variability.
At the individual level, in the sensor-space ATM+SVM yielded a statistically better classification accuracy than CSP+SVM for 9 subjects. In 8 subjects, CSPs yielded better accuracy than ATMs. In 3 subjects, there was not any statistically significant difference between the two approaches *(Fig. 1B)*. In the source-space, ATM+SVM yielded significantly higher classification accuracy than CSP+SVM for 13 subjects, while the opposite was true for 4 subjects. For the remaining 3 subjects, there was not any statistically significant difference between the decoding performances of the two approaches *(Fig. 1E)*.

To investigate the possibility to reduce the computational time to get closer to a configuration more compatible with the online requirements, we investigated the accuracy performance across different random splits configurations (5, 25, 50, 75) both at the individual and at the group level. As shown in *Fig. 1A & D* the performance was robust across splits for both CSP+SVM and ATM+SVM pipelines (one-way ANOVA p>0.05), and we observed a higher accuracy score for most of the subjects with 5 splits both in sensor and source space. Based on the observations made on the inter-subject variability, we validated the significant difference of the variance of these two populations via the F-test (pval<0.05). The statistical difference between the two pipelines was achieved both in the sensor and in the source space.
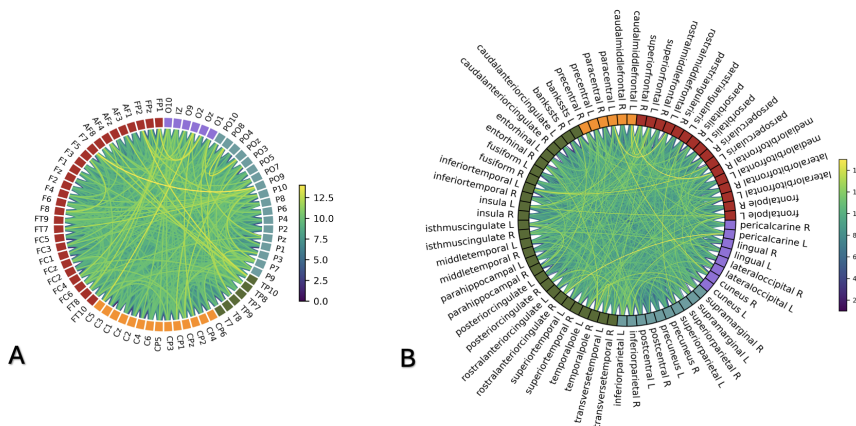
Figure 2: Features selection.

(A) *Edges-wise, valid at group level in sensor-space*

(B) *Edges-wise, valid at group level in source-space*

When considering 5 splits, at the group level, in the sensor space, no significant difference was observed between the two pipelines (t-test, p-value > 0.05) but CSP+SVM (72% +/- 15.55%) showed a larger inter-subject as compared to ATM + SVM (73% +/- 9.14%).

In the source space, ATM + SVM (81% +/- 7.5%) led to a statistical improvement of the performance (t-test, pval<0.01) as compared to CSP + SVM (75% +/- 14%) and a significant reduction of inter-subject variability.

At the individual level: in the sensor-space *(Fig.1C)*, with 5 splits, ATM+SVM yielded a statistically better classification accuracy than CSP+SVM for 9 subjects. In 7 subjects, CSPs yielded better accuracy than ATMs and in four subjects, there was not any significant difference between the two approaches. However, CSP+SVM pipeline led to a larger number of subjects with a performance below the chance level, set to 58% here [13] (6 subjects) than with ATM+SVM (1 subject). In the source space, ATM+SVM showed an improved performance in 12 subjects, while the opposite was true for 3 subjects with CSP+SVM *(Fig. 1F)*.

From now on, unless specified otherwise, the chosen configuration will involve 5 splits to closely mimic a real-time setup, and the subsequent sections will deal with ATM data only.

Sensor and source space selected features
To investigate the interpretability of the decoding performance, we estimated the weights attributed to each feature. A preliminary probabilistic analysis showed that most of the selected features presented a lower feature importance and that only a few were notably higher, suggesting that only a reduced number of features were relevant. When considering the features selected in at

least half of the cohort, an edge involving left central electrodes (C5) and occipital electrodes (O2) was obtained in 13 subjects *(Fig. 2A)*. We observed a predominant involvement of left central electrodes connected to occipital electrodes, between left and right central electrodes connected to parietal electrodes.

Similar observations were possible in the source-space. Looking for a recurrent path across most of the subjects, see *Fig 2B*, in 15 subjects, most of the connections involved left paracentral, rostral anterior cingulate cortex, caudal middle frontal gyrus and medial lateral orbito-frontal regions.

These interactions correspond to edge clusters that were task-dependent and consistent across subjects in encoding investigation shown in our previous paper [7]. Moreover, the features with higher weight often involved the left paracentral and the precentral areas.

To get a more synthetic vision of these results, we performed a similar analysis at the nodal level, confirming the results previously obtained. To increase the statistical validity of such observations, in this part, we worked with the 50-split configuration. In the sensor-space, the electrodes with highest features' importance were C5 and P8. Nevertheless, it is possible to observe a general activation in electrodes over the bilateral motor cortex, and the bilateral parietal lobe. In the source-space, the most frequently selected brain regions were the right paracentral area, the left frontal pole and the right rostral anterior cingulate.

Encoding-Decoding Match in sensor-space
To investigate the neurophysiological validity of the selected features, we compared them with the results obtained with an encoding framework. To achieve this,
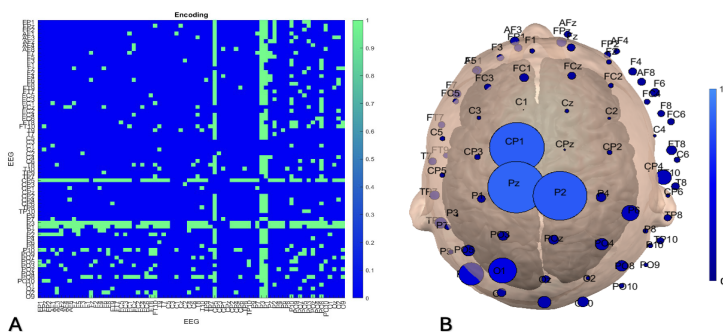

Figure 3: Encoding analysis in sensor-space.

(A) *Encoding reliably different edges cluster at group level in sensor-space*

(B) *Encoding at nodal and group level in sensor-space*

we examined differences between the two experimental conditions in the probabilities of perturbations propagating across two brain regions. Our results show that there is a set of links over CP and P electrodes (CP5, P1, P2 edges-wise and CP1, Pz, P2 at nodal level), in which the difference between two conditions (MI and rest) was consistently significant across most of the subjects (p < 0.0001, BH corrected) *(Fig. 3A/B)*.

Following the features' importance analysis described in the previous section, we performed a quantitative reliability analysis to consider only the edge-wise selected in at least half of the subjects *(Fig. 2A)*. The final goal of this analysis was the comparison between reliably different edges selected in the encoding phase and the features selected in most subjects with the larger attributed weight. Indeed, we observed a higher level of match score with the ten subjects with a highest classification performance (37%, see *Fig. 4A)* as compared to the ten subjects with the lowest classification performance *(6%, see Fig. 4B)* but also to the entire dataset *(9%, see Fig. 4C)*.

A. B. C.
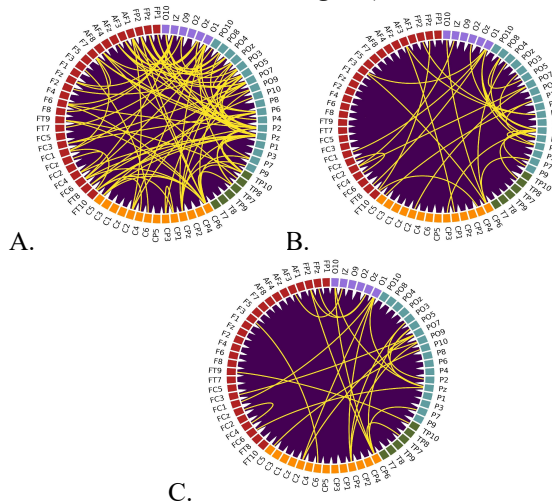
Figure. 4: Edges matches between encoding and decoding: (A) *Results obtained from the ten subjects with the highest classification performance;* **(B)** *Results obtained from the ten subjects with the lowest classification performance;* **(C)** *Results obtained from the entire dataset.*

DISCUSSION

In the sensor space as well as in the source space, the classification of ATMs led to an improvement of the decoding performance with respect to the benchmark (namely the spatial filter-based approach) in most of the subjects robustly across the different number of tested random splits. Importantly, in both source and sensor domains, we observed a reduced intra and inter-subject variability with ATM+SVM as compared to CSP+SVM. These findings suggest that the use of our approach could be a tool to reduce the BCI inefficiency phenomenon.

Beyond the classification performance, we also investigated the interpretability of our findings through the study of the selected features. ATMs present a straightforward interpretability as opposed to CSPs, which operate on large-scale components of the signal that are not as readily interpretable. Indeed, it is possible to study and to identify the selected features at the subject level but a quantitative analysis at the group level is not applicable because of the difficulty to identify a common precise pattern across different subjects and different selected features. At the individual level, the information captured by the two types of feature extraction (namely CSPs and ATMs) are complementary, as seen in Fig. 5. ATMs is based on edge-wise representations and focus on strong coherent interactions that intermittently occur on the large-scale whereas CSP features, that embedded pipelines based on techniques that assume stationarity, rely on local measurements (mostly frequency band power features and time-point features) disregarding the propagation of brain dynamics at consecutive time instants.

To further study the meaning of the features selected with ATMs, we adopted an encoding framework identified here as a set of functional connections (i.e., edges) that consistently exhibited a higher likelihood of dynamic recruitment during a hand motor imagery task as compared to the resting state at the group level. This straightforward approach, validated on the entire dataset, allowed us to reliably extract functional information specific to the task execution at the individual level, an observation not achievable through traditional functional metrics (namely power spectra and phase-locking value) [7]. Therefore, from a theoretical standpoint, our study establishes the foundation for exploring neuronal avalanche metrics as a novel functional connectivity measure for investigating changes during motor tasks based not on the functional activation between two brain areas at the same time but on consecutive activations.
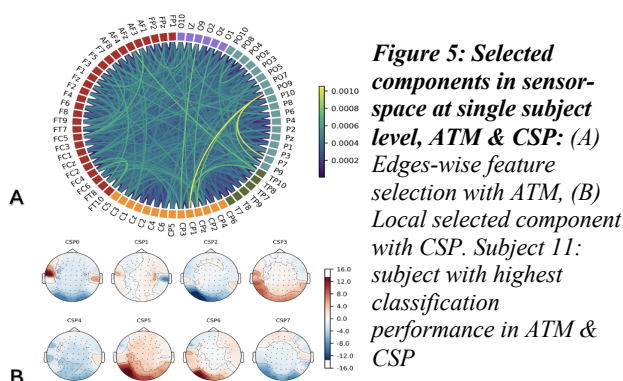
In the sensor space, the electrodes that showed a higher feature importance, identified through the decoding framework, were located over the same brain areas defined as "reliably edges" in the encoding framework. Moreover, we noticed that an increased match between the selected features and the edges-clusters led to an improvement of the classification performance. This finding suggests a possible way to apply a dimensionality reduction in the features used in the decoding step, to improve the classification performance. An ongoing work consists in investigating the key-parameters of the neuronal avalanches to be tuned and the associated features selection approaches to assure that the most relevant information will be considered for the classification step. Considering such approaches will improve the performance, but they will also reduce the computational time as well; two key-aspects of the feasibility of our pipeline in real-world scenarios.

In our work, to emphasise this possible future development, we dealt with epochs of 5s from which 25ms and 27ms (respectively for ATM + SVM and CSP+SVM) were required to extract the features and to perform the classification. Such computational time estimations are in line with current real time settings that rely on similar time windows and propose an update of the provided feedback every 28 ms. Future work will consist in identifying strategies to extract neuronal

avalanches, and therefore ATMs, in shorter time windows to make our framework completely compatible with online settings.

To further investigate the physiological meaning of our findings we compared the results respectively obtained in the sensor and in the source space. The most frequently selected features involved central electrodes (C-CP) in the sensor-space, and the paracentral area in the source-reconstructed data, implying the motor-area. Moreover, our results showed that other networks were involved in a motor-imagery task, through the selection of electrodes above parietal and occipital areas. The parietal lobe is structurally divided into inferior parietal lobe, superior parietal lobe, and precuneus [14]; its principal functions are the perception of the body, the integration of somatosensory information (e.g. touch, pain, pressure and temperature), visuospatial processing and coordination of movement. As such, the parietal activation is in line with our observations [7], because the subjects were instructed to perform a kinesthetic motor imagery task, that involves imagining movements as well as sensing the touch caused by the grasped object, and because coordinating hand, arm, and eye motions is required to perform our task. A similar role of precuneus in coordination of motor behaviour is achieved by anterior cingulate cortex [13] and its involvement has come to light in source-reconstructed data [7]. The occipital lobe [15] is primarily responsible for visual processing. Its recurrent activation and connection with central electrodes usually happens during a kinesthetic task, and when a visual stimulation is proposed as it was during our experiments.

Moreover, mainly in the source-space, we observed the involvement of the caudal portion of the middle frontal gyrus and of the medial-orbital frontal area. Within the caudal portion of the middle frontal gyrus, at the intersection with the precentral gyrus, is the frontal eye fields (Brodmann area 8). The frontal eye fields control saccadic eye movements, rapid, conjugate eye movements that allow the central vision to scan numerous details within a scene or image, same meaning of orbital regions involvement [16], instead medial-orbital frontal region reflects the allocation of attentional resources, which are typically engaged in cognitive/motor tasks [7]. Such findings demonstrate the neurophysiological validity of the selected features.

Figure 5: Selected components in sensor-space at single subject level, ATM & CSP: (A) Edges-wise feature selection with ATM, (B) Local selected component with CSP. Subject 11: subject with highest classification performance in ATM & CSP

CONCLUSION

Our results suggest that the integration of periodic and aperiodic features would be a straightforward way to capture functionally relevant processes, in turn, to apply them to the design of BCIs and to improve task classification. The good performance of the ATMs on the EEG data in the sensor space is relevant to translate our methodology to real-world scenarios. Until now, we tested this new feature only during a hand motor imagery BCI task. Future work will consist in considering a wider range of BCI paradigms for communication and movements recovering applications.

REFERENCES

[1] Alwi Alkaff, *et al.* Applications of Brain Computer Interface in Present Healthcare Setting. in *Artificial Intelligence* vol. **0** (IntechOpen, 2024).

[2] Allison, B. Z. & Neuper, C. Could Anyone Use a BCI? in *Brain-Computer Interfaces* (eds. Tan, D. S. & Nijholt, A.) 35–54 (2010).

[3] Lotte, F. *et al.* A Review of Classification Algorithms for EEG-based Brain-Computer Interfaces: A 10-year Update. *J. Neural Eng.* (2018)

[4] Arviv, O. *et al.*. Neuronal avalanches and time-frequency representations in stimulus-evoked activity. *Sci. Rep.* **9**, 13319 (2019).

[5] Sorrentino, P. *et al.* The structural connectome constrains fast brain dynamics. *eLife* **10**, e67400 (2021).

[6] Rabuffo, G., *et al.* Neuronal Cascades Shape Whole-Brain Functional Dynamics at Rest. *eNeuro* **8**, ENEURO.0283-21.2021 (2021).

[7] Corsi, M.-C. *et al.* Measuring brain critical dynamics to inform Brain-Computer Interfaces. iScience **27**, 108734 (2024)

[8] Corsi, M.-C. *et al.* Functional disconnection of associative cortical areas predicts performance during BCI training. *NeuroImage* **209**, 116500 (2020).

[9] Koles, Z.J., *et al.* Spatial patterns underlying population differences in the background EEG. *Brain Topogr.* **2**, 275–284 (1990).

[10] Blankertz, B., *et al.* Optimizing Spatial filters for Robust EEG Single-Trial Analysis. *IEEE Signal Process. Mag.* **25**, 41–56 (2008).

[11] Shriki, O., *et al.* Neuronal Avalanches in the Resting MEG of the Human Brain. Journal of Neuroscience, 33 (16) 7079-7090.

[12] Benjamini, Y., and Hochberg, Y. Controlling the False Discovery Rate: A Practical and Powerful Approach to Multiple Testing. J. R. Stat. Soc. Ser. B Methodol. **57**, 289–300 (1995).

[13] Müller-Putz, *et al.* G. Better than random? A closer look on BCI results. International Journal of Bioelectromagnetism (2008).

[14] Wenderoth, N., *et al.* The role of anterior cingulate cortex and precuneus in the coordination of motor behaviour. *Eur. J. Neurosci.* **22**, 235–246 (2005).

[15] Kwon, S., *et al.* Neuropsychological Activations and Networks While Performing Visual and Kinesthetic Motor Imagery, *Brain Sci.* **2023**, *13*, 983.

[16] Schall J.D., Frontal Eye Fields, *Encyclopedia of Neuroscience.* Pages 367-374 (2009).